

Geochemical tracers of buried estuary of Rushikulya River from Odisha, east coast of India

Saju Varghese*, Subhasis Roychaudhuri, P. A. Mohammed Mashood and Sachin Tripathi

Marine and Coastal Survey Division, Geological Survey of India, Kolkata 700 091, India

The sediments of the inner to middle shelf region of the central part of the east coast of India immediately near the growing spit of the Rushikulya River mouth, are characterized by very hard, compact, dark gray clayey silt and clay with medium to coarse sand and wood piece layers at different levels. Maximum output of the Rushikulya River during monsoon season is marked by thin layers of coarse to medium sand at different subsurface levels below the sea floor within the inner to middle shelf areas. Geochemical analysis (major and trace elements) of seabed sediments shows significant correlation with aluminium. Variation in other elements, except calcium and barium confirm their association with aluminosilicate minerals. The higher concentration of Ti-rich heavy minerals near the coast in front of the Rushikulya River is inferred due to terrigenous supply by the river. The REE analysed in the carbonaceous clays indicates enrichment of Σ REE in the sediments, which is interpreted as due to the absorption of REE into the lattices of clay from sea water. Intermittent layers of carbonaceous clay with abundant wood pieces along with the presence of H_2S and the enrichment of REE in the clay provide indirect evidences for the presence of a buried estuary in front of the Rushikulya River at different subsurface levels. The growing spit towards the northeast direction at the river mouth further acts as a favourable geomorphologic feature for the formation of an estuary in the study area. Presence of a reworked palaeo-sand ridge located between 54 and 57 m water depth is characterized by selective elimination of elements from the sediments. Furthermore, this sand ridge acts as the boundary for the buried estuary identified in the study area.

Keywords: Estuary, geochemical analysis, sand ridge, sedimentological studies.

GEOCHEMICAL studies of marine sediments are especially helpful in understanding the different sediment sources, element distribution pattern and evaluating the environmental conditions existing in an area. Further, the shal-

low sediments record information on sea-level changes. Studies using seismic reflection profiles are a potential tool to identify sequences and then using them to estimate the ages and magnitudes of past sea-level changes^{1,2}. However, this method is highly controversial, in part because of the proprietary nature of the data used to construct it and in part because of the flaws in the method used to estimate the amplitude of sea-level changes. Further, oxygen isotope ratios ($\delta^{18}O$) provide a potential means for reconstructing sea-level changes over the past 100 Myr. Comparison of the sequence stratigraphic record with oxygen isotopes provides a link between regional sea-level lowerings and global changes in ice volume for the past many million years. In the Indian context, glacio-eustatic sea-level changes during late Quaternary have left various significant signatures on the coastal areas as well as inner part of continental shelves such as three different still stands at 30, 100 and 120 m (refs 3–5). Despite the efforts to document the distribution of major and trace elements along the east and west coast shelf sediments, identifying the factors responsible for major and trace elements distribution in coastal sediments requires vigorous geochemical studies due to different environmental settings and the resulting sediment characteristics from region to region^{6–12}. Although many geochemical studies have been carried out on the shelf and slope sediments of the southwest coast of India^{11,13–15}, an integrated geochemical study incorporating major and trace element and REE composition of shelf areas has not been carried out so far in the east coast of India. This article reports the major and trace elements composition of selected nearshore sediments at the confluence of the Rushikulya River Odisha with the sea.

Methods

To geochemically characterize the various features associated with glacio-eustatic sea-level changes off Rushikulya River (Figure 1), the methodologies adopted include characterization of the behaviour of major and trace elements, including REE in the surface sediments and the cores, and evaluation of the spatial distribution of major

*For correspondence. (e-mail: saajuvarghese@gmail.com)

and trace elements in the studied samples collected during the ST-223 cruise on-board *R. V. Samudra Kaustubh*. The sediments from the survey area were collected using a sampler (Van Veen Grab and vibro corer). Immediately after collection, the samples were kept frozen till they were brought to the laboratory for further studies. After logging the core, fractions from surface samples and sub-samples from two vibro cores were selected for geochemical studies. Next, 20 g of air-dried sub-samples was desalinated thrice using distilled water before chemical treatment for major and trace elements analysis. The samples were crushed in an agate mortar until the entire quantity passed through $-120 + 100$ ASTM mesh size. For element analysis, a known quantity of the powdered samples was digested with a mixture of concentrated hydrofluoric acid–nitric acid–perchloric acid following the method of Zhang and Liu¹⁶. A fraction (~ 0.25 g) from each sub-sample was treated with aqua regia (to dissolve the iron in the sediments) followed by treatment with hydrofluoric acid to remove the silicates. Perchloric acid was used to remove the organic content in the sediments before the samples were made up to a 100 ml solution using dilute nitric acid. The samples in the nitric medium were subjected to major oxides and trace elements analysis (Varian 720-ES Inductively coupled plasma optical emission spectrometer; ICP-OES). Based on the parallel analysis of international reference material and in-house standards to monitor the accuracy of the analytical methods, the analytic precision of major and trace elements was found to be better than 5% and 10% respectively, for the analysed samples. Loss on ignition (LOI) was analysed on ignition in a muffle furnace at 1000°C , while P_2O_5 was determined by colour development with ammonium molybdate–ammonium metavanadate solutions with subsequent measurement using a spectrophotometer at 465 nm. Contents of major oxides and trace elements were reported as analysed, not on a carbonate-free basis. Tables 1 and 2 provide the results of analysis of major oxides and

trace elements for surface as well as down the cores of VC-05 and VC-06 respectively. Table 3 provides results of REE analysis of the carbonaceous clay from VC-05.

Correlation of major oxides and trace elements separately and together as well as principal components analysis (PCA) were carried out to analyse the geochemical data by creating factors (new variables) which represent clusters of interrelated variables. PCA analysis is a multivariate method which can explain the major variations within a dataset. The analysis enables a reduction in data and description of complex systems by means of a small number of components. Each component is a weighted, linear combination of the original variables. PCA analysis of VC-05 was performed using XLSTAT, an add-in software package for Microsoft Excel (Addinsoft Corp.).

Results

Bathymetry and sedimentology

The coastline in the study area is fairly straight trending $\text{N } 40^{\circ}\text{--}50^{\circ}$, and a narrow spit of about 2 km length growing in the direction of the longshore current marks the Rushikulya confluence with the sea. It is apparent from the bathymetric contour map that the seafloor in the inner shelf region of this area is almost smooth with gentle slope and a submerged ridge within the present study area in the depth range 54–57 m (Figure 2). In general, grain size in the shallow region (up to 30 m water depth) is primarily sandy in nature, while the deeper part of the sediment column is dominated by silty to sandy silty sediments. The sediments of VC-5 are characterized by alternating layers of sand and mud from top to bottom, with smell of sulphur at the time recovery, layers consisting wood pieces and sand towards the bottom (Figure 3). Exactly in front of the river mouth in VC-6, the top portion of the sediment column (up to ~ 50 cm) is light brown, coarse to very coarse sand with profuse shell fragments (complete bivalve shells), which in turn change to silty clay layers admixed with medium to coarse sand patches containing abundant shell fragments at different levels (Figure 3). XRD analysis of the surface sample of the cores collected shows quartz as the major mineral with small amounts of mica, kaolinite, K-feldspar and trace amounts of calcite, plagioclase and chlorite.

Dispersion of major oxides

The surface distribution of major oxides follows a general increasing trend towards deeper waters, except MnO and TiO_2 as they show a rather inverse pattern (Table 1). The central part of the area from where GC/07 was collected, shows a low value for all the oxides (Table 1). Al_2O_3 concentration in seabed surface sediment varied from 3.29% to 17.76% in the coast and from 3.53% to

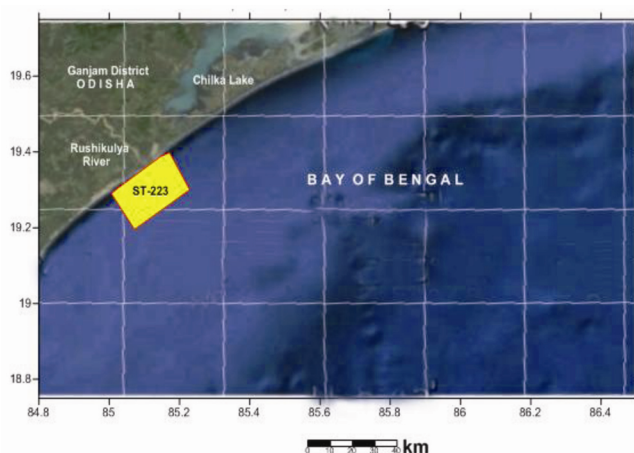


Figure 1. Location map of the study area off Rushikulya River, Odisha, India.

Table 1. Representative major oxide analysis of surface sediments and vibro cores VC-05 and VC-06, off Rushikulya River, Odisha, India

Sample	Al ₂ O ₃ (%)	Fe ₂ O ₃ (%)	MgO (%)	CaO (%)	MnO (%)	Na ₂ O (%)	K ₂ O (%)	TiO ₂ (%)	P ₂ O ₅ (%)	Loss on ignition (%)
Surface distribution of major oxides										
ST-223/G/1	18.64	8.76	2.39	1.46	0.06	1.44	2.67	0.97	0.14	15.07
ST-223/VC/2	4.89	5.45	0.64	1.43	0.09	0.50	0.99	2.68	0.06	1.43
ST-223/VC/3	5.31	7.08	0.75	1.42	0.13	0.70	0.44	3.93	0.09	1.22
ST-223/VC/4	15.61	7.66	1.87	1.96	0.07	0.94	1.47	1.03	0.13	11.81
ST-223/VC/5	6.37	4.42	0.88	4.88	0.05	0.53	0.59	1.43	0.07	5.73
ST-223/VC/6	3.53	1.91	0.38	1.70	0.04	0.56	0.16	0.96	0.03	1.74
ST-223/GC/7	3.29	1.41	0.45	0.28	0.04	0.42	0.12	0.25	0.02	13.50
ST-223/GC/8	17.01	8.33	2.17	1.77	0.06	0.81	1.82	0.97	0.16	14.28
ST-223/GC/9	16.95	8.29	2.11	1.46	0.06	0.77	1.92	0.90	0.14	13.88
ST-223/GC/10	16.89	8.29	2.06	1.21	0.06	0.70	0.96	0.91	0.14	14.68
ST-223/GC/11	4.21	1.77	0.61	0.15	0.04	1.16	0.12	0.26	0.02	14.63
ST-223/GC/12	18.25	8.96	2.34	1.45	0.06	0.90	1.50	0.94	0.16	14.73
ST-223/GC/13	17.76	8.66	2.35	1.78	0.06	0.80	1.75	0.89	0.14	15.17
Down core Variation of major oxides from VC-05 and VC-06										
ST-223/VC/5/1	15	20	75	85	10	<5	490	240	190	65
ST-223/VC/5/2	12.82	5.24	1.48	0.42	0.02	0.87	1.68	0.76	0.04	17.51
ST-223/VC/5/3	13.92	6.58	1.65	0.59	0.03	0.98	2.26	0.88	0.08	18.73
ST-223/VC/5/4	15.77	7.02	1.79	0.52	0.04	1.21	2.77	0.89	0.09	16.04
ST-223/VC/5/5	16.82	7.01	1.93	0.40	0.03	0.78	2.42	0.83	0.10	17.11
ST-223/VC/5/6	16.68	8.37	1.90	0.42	0.03	1.04	3.08	0.83	0.10	18.86
ST-223/VC/5/7	15.40	7.95	1.78	0.39	0.04	1.13	2.12	0.80	0.10	19.47
ST-223/VC/5/8	16.05	8.16	1.95	0.45	0.04	1.13	2.12	0.80	0.10	19.47
ST-223/VC/5/9	17.18	8.49	2.16	1.41	0.06	0.72	1.43	0.93	0.16	20.45
ST-223/VC/5/10	15.32	7.69	1.90	0.45	0.03	0.86	2.08	0.71	0.10	22.18
ST-223/VC/5/11	15.83	6.83	1.78	0.45	0.03	1.01	2.48	0.85	0.10	16.44
ST-223/VC/5/12	15.51	8.20	1.59	0.35	0.03	0.60	1.61	0.75	0.09	17.75
ST-223/VC/5/13	14.72	7.10	1.57	0.53	0.03	0.99	2.84	0.82	0.11	13.50
ST-223/VC/6/1	3.53	1.91	0.38	1.70	0.04	0.56	0.16	0.96	0.03	1.74
ST-223/VC/6/2	6.38	2.41	0.78	1.37	0.02	0.56	1.20	0.59	0.05	3.41
ST-223/VC/6/3	5.79	2.53	0.59	1.32	0.03	0.72	1.47	1.14	0.05	2.38
ST-223/VC/6/4	6.72	2.83	0.83	2.91	0.03	0.64	1.61	0.76	0.04	4.50
ST-223/VC/6/5	7.26	3.21	0.73	1.31	0.03	0.72	2.28	1.14	0.04	3.38
ST-223/VC/6/6	11.32	5.20	1.24	1.05	0.03	0.75	2.28	0.96	0.07	9.57
ST-223/VC/6/7	13.61	6.89	1.65	1.19	0.08	1.34	1.81	0.84	0.09	14.75
ST-223/VC/6/8	11.08	5.23	1.23	2.30	0.06	0.97	1.56	0.84	0.07	9.18
ST-223/VC/6/9	15.65	7.91	2.29	1.99	0.05	0.98	1.49	0.84	0.10	12.70

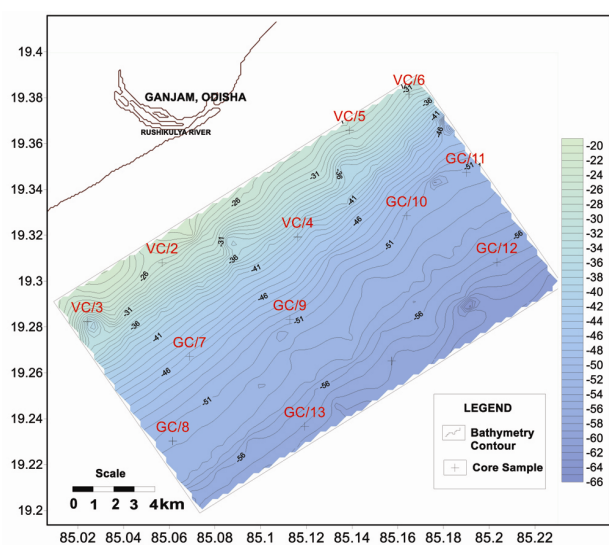


Figure 2. Map showing the bathymetry and sample location of the study area.

17.18% in the subsurface. In surface sediments, Fe₂O₃ content was generally found ranging from 1.41% to 8.96%, while down the core it increased gradually from the top (1.91%) to bottom (8.49%). On the seafloor, MgO concentration in seabed sediments increased with water depth, i.e. from 0.38% to 2.35%, whereas its concentration range varied from 0.38% to 2.29% from top to bottom of the core. CaO showed a variation from 0.15% to 4.88% on the seafloor and 0.15% to 2.30% down sediment column of the present study area. On the other hand, MnO variation was less conspicuous (from 0.04% to 0.13% on seabed sediments and from 0.02% to 0.08% down the sediment column). Na₂O and K₂O varied from 0.42% to 1.44% and 0.12% to 2.67% on seabed sediments, and 0.53% to 1.34% and 0.16% to 3.16% in subsurface sediments respectively. TiO₂ content decreased from shallow (3.93%) to deeper parts (0.25%) in the surface sediments, while in the down core sediment column it varied from 0.59% to 1.14%. P₂O₅ content in surface sediments

Table 2. Representative minor element analysis of surface sediments and vibro cores VC-05 and VC-06, off Rushikulya River

Sample	Cu (ppm)	Pb (ppm)	Zn (ppm)	Ni (ppm)	Co (ppm)	Cd (ppm)	Ba (ppm)	Sr (ppm)	Cr (ppm)	V (ppm)
Surface distribution of minor elements										
ST-223/G/1	45	30	205	70	30	<5	380	105	125	120
ST-223/VC/2	15	50	75	25	10	<5	505	100	75	66
ST-223/VC/3	10	70	105	70	15	<5	190	105	135	100
ST-223/VC/4	35	75	155	65	25	<5	530	125	150	95
ST-223/VC/5	15	20	75	85	10	<5	490	240	190	65
ST-223/VC/6	10	10	25	40	5	<5	440	90	50	30
ST-223/GC/7	5	10	15	5	5	<5	95	15	20	20
ST-223/GC/8	35	115	185	70	25	<5	430	110	100	105
ST-223/GC/9	35	75	175	60	30	<5	440	95	135	105
ST-223/GC/10	35	75	175	70	25	<5	400	90	110	110
ST-223/GC/11	15	10	15	25	5	<5	120	20	55	30
ST-223/GC/12	40	115	200	65	30	<5	380	95	125	120
ST-223/GC/13	40	55	185	70	30	<5	375	105	105	115
Down core variation of minor elements from VC-05 and VC-06										
ST-223/VC/5/1	15	20	75	85	10	<5	490	240	190	65
ST-223/VC/5/2	30	15	135	45	20	<5	215	60	90	85
ST-223/VC/5/3	30	30	130	55	20	<5	420	75	80	95
ST-223/VC/5/4	35	30	165	60	20	<5	465	75	155	120
ST-223/VC/5/5	35	30	160	45	25	<5	405	70	105	105
ST-223/VC/5/6	45	20	180	65	30	<5	270	70	125	105
ST-223/VC/5/7	35	25	140	65	25	<5	365	65	75	95
ST-223/VC/5/8	40	25	170	65	25	<5	365	70	185	115
ST-223/VC/5/9	40	120	170	75	30	<5	385	100	95	110
ST-223/VC/5/10	35	25	150	55	20	<5	370	75	105	95
ST-223/VC/5/11	35	35	150	55	20	<5	425	75	95	90
ST-223/VC/5/12	35	20	135	55	25	<5	395	60	90	105
ST-223/VC/5/13	30	20	135	55	25	<5	540	80	100	95
ST-223/VC/6/1	10	10	25	40	5	<5	440	90	50	30
ST-223/VC/6/2	10	10	40	20	5	<5	525	100	50	35
ST-223/VC/6/3	10	15	40	20	5	<5	560	95	60	40
ST-223/VC/6/4	15	5	60	25	5	<5	555	130	55	40
ST-223/VC/6/5	25	20	70	20	10	<5	645	105	50	45
ST-223/VC/6/6	20	30	85	40	15	<5	625	95	95	65
ST-223/VC/6/7	30	35	125	55	25	<5	470	90	85	90
ST-223/VC/6/8	20	20	100	30	15	<5	525	125	75	65
ST-223/VC/6/9	30	35	155	60	20	<5	410	115	75	100

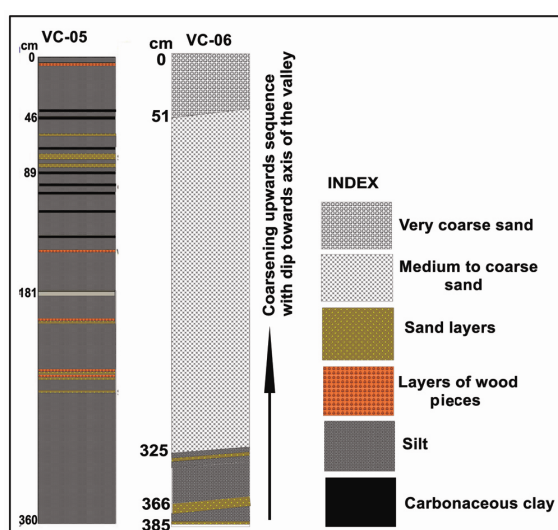


Figure 3. Downcore variation of the cores VC-05 and VC-06. VC-05 depicts different layers of sand, carbonaceous clay and wood pieces, whereas VC-06 shows a coarsening upward sequence.

varied between 0.04% and 0.16% and down the core it ranged from 0.03% to 0.16%. LOI varied from 1.22% to 15.17% in seabed sediments and 1.74% to 22.18% down the sediment column of cores.

Distribution of trace elements

Distribution of trace elements revealed that Cu content in sediments varied widely from 5 to 45 ppm, while down the sediment column it increased gradually with depth from 10 to 45 ppm. The concentration of lead on the sea-floor varied from 10 to 115 ppm, whereas down the core in the sediment column it (varies from 5 to 120 ppm) showed almost the same values except a major nick at 2 m level in GC/05, whereas in GC/6 it gradually increased down the core. Zn content varied from 15 to 205 ppm on the sea floor and 25 to 200 ppm in down-core sediment column. On the seafloor, Ni and Co values varied from 5 to 85 ppm and 5 to 30 ppm respectively, while down the

RESEARCH ARTICLES

Table 3. Concentration of REE in carbonaceous clay from the mouth of Rushikulya River

Sample no	La	Ce	Pr	Nd	Eu	Sm	Gd	Tb	Dy	Ho	Er	Tm	Yb	Lu	ΣREE
VC/5/1	46.27	84.97	9.89	34.38	1.40	6.56	7.12	1.00	5.90	1.13	3.34	0.54	3.31	0.54	206.36
VC/5/2	45.64	84.21	9.77	33.41	1.38	6.51	7.17	1.05	6.10	1.18	3.43	0.56	3.43	0.53	204.38
GC/5/3	67.00	118.48	14.26	49.83	1.92	9.55	9.23	1.24	6.93	1.30	3.77	0.61	3.74	0.60	288.45
GC/5/4	57.01	106.24	12.11	42.56	1.68	8.09	8.01	1.09	6.06	1.11	3.17	0.53	3.26	0.50	251.42
GC/5/5	57.06	106.07	12.10	42.33	1.67	8.24	7.91	1.08	5.84	1.06	3.09	<0.50	3.23	0.50	250.19
GC/5/6	55.51	104.17	11.93	40.58	1.63	7.84	7.80	1.07	6.02	1.12	3.26	0.53	3.24	0.52	245.22
GC/5/7	52.90	97.55	11.29	39.78	1.55	7.36	7.52	1.05	5.82	1.08	3.18	0.52	3.20	0.52	233.31
GC/5/8	53.65	98.31	11.31	39.94	1.56	7.37	7.25	1.00	5.53	1.01	2.92	<0.50	2.95	<0.50	232.78
GC/5/9	55.41	103.16	11.88	41.33	1.63	7.86	7.76	1.07	5.99	1.11	3.23	0.53	3.22	0.50	244.69
GC/5/10	50.77	94.37	10.84	37.23	1.49	7.15	7.06	0.99	5.41	0.99	2.86	<0.50	2.89	<0.50	222.05

Table 4. Correlation matrix of major oxides from VC-05

	Al ₂ O ₃	Fe ₂ O ₃	MgO	CaO	MnO	Na ₂ O	K ₂ O	TiO ₂	P ₂ O ₅	LOI
Al ₂ O ₃	1									
Fe ₂ O ₃	0.849779	1								
MgO	0.942745	0.826628	1							
CaO	-0.8518	-0.61091	-0.71403	1						
MnO	-0.13955	0.135841	0.06087	0.56916	1					
Na ₂ O	0.471361	0.316014	0.442194	-0.58632	-0.21327	1				
K ₂ O	0.667226	0.443482	0.529859	-0.73164	-0.47403	0.760583	1			
TiO ₂	-0.80168	-0.61642	-0.68292	0.967173	0.57825	-0.45589	-0.59853	1		
P ₂ O ₅	0.575541	0.714483	0.664515	-0.12704	0.602451	0.029853	0.156681	-0.112	1	
LOI	0.813852	0.741705	0.856463	-0.79497	-0.19377	0.385356	0.391395	-0.836	0.351754	1

LOI, Loss on ignition.

Table 5. Correlation matrix of trace elements from VC-05

	Cu	Pb	Zn	Ni	Co	Ba	Sr	Cr	V
Cu	1								
Pb	0.29394	1							
Zn	0.956886	0.325971	1						
Ni	-0.23566	0.365173	-0.29248	1					
Co	0.87074	0.400674	0.799645	-0.17746	1				
Ba	-0.45762	0.04605	-0.37677	0.260309	-0.3275	1			
Sr	-0.75023	0.050726	-0.72937	0.746497	-0.6616	0.415508	1		
Cr	-0.23926	-0.16654	-0.14434	0.55102	-0.3890	0.229516	0.581832	1	
V	0.805712	0.301317	0.858778	-0.20998	0.70298	-0.08705	-0.65087	-0.0050	1

Table 6. Correlation matrix of major oxides from VC-06

	Al ₂ O ₃	Fe ₂ O ₃	MgO	CaO	MnO	Na ₂ O	K ₂ O	TiO ₂	P ₂ O ₅	LOI
Al ₂ O ₃	1									
Fe ₂ O ₃	0.990335	1								
MgO	0.972291	0.971723	1							
CaO	-0.03402	-0.03496	0.056706	1						
MnO	0.64111	0.705321	0.587109	0.036323	1					
Na ₂ O	0.813043	0.840803	0.740331	-0.11408	0.919558	1				
K ₂ O	0.483811	0.399737	0.345006	-0.22172	0.028078	0.353555	1			
TiO ₂	-0.18338	-0.13613	-0.26376	-0.36412	-0.07336	-0.03448	0.228151	1		
P ₂ O ₅	0.969476	0.967451	0.957652	-0.11505	0.658365	0.822661	0.354373	-0.215	1	
LOI	0.960346	0.96587	0.914519	-0.05778	0.77384	0.890899	0.39875	-0.238	0.943547	1

core in the sediment column Ni content varied from 20 to 60 ppm and Co content from 5 to 30 ppm. Ba content varied from 95 to 505 ppm on the seafloor and 215 to 645 ppm in sediment column down the cores. In the study area, Sr content varied widely from 15 to 240 ppm, while on the seafloor, it varied from 60 to 130 ppm. Dis-

person of Cr in seabed sediments varied from 20 to 190 ppm, whereas in subsurface sediments it varied from 50 to 155 ppm. V content varied from 20 to 120 ppm on the seafloor and 30 to 120 ppm in sediment column down the core. Cd content of less than 5 ppm was seen in all types of sediments, irrespective of their texture (Table 2).

Table 7. Correlation matrix of trace elements from VC-06

	Cu	Pb	Zn	Ni	Co	Ba	Sr	Cr	V
Cu	1								
Pb	0.851394	1							
Zn	0.914151	0.859085	1						
Ni	0.666479	0.76738	0.754163	1					
Co	0.896889	0.931695	-0.33383	0.798944	1				
Ba	-0.1382	-0.18757	0.91021	-0.67335	-0.30072	1			
Sr	0.126918	-0.22361	0.261951	-0.16342	-0.05556	0.03693	1		
Cr	0.572758	0.809699	0.687809	0.630673	0.796474	-0.0265	-0.09853	1	
V	0.878274	0.916788	0.97892	0.827997	0.95	-0.3925	0.091667	0.76363	1

Table 8. Factor loadings for the major oxides and trace elements for the cores VC-05

	F1	F2
Al ₂ O ₃ (%)	0.838	0.470
Fe ₂ O ₃ (%)	0.752	0.256
MgO (%)	0.850	0.445
CaO (%)	-0.066	0.170
MnO (%)	0.035	-0.414
Na ₂ O (%)	0.799	-0.149
K ₂ O (%)	0.895	0.218
TiO ₂ (%)	-0.189	-0.498
P ₂ O ₅ (%)	0.754	0.435
LOI (%)	0.635	0.424
Cu	-0.664	0.701
Pb	0.054	0.493
Zn	-0.624	0.714
Ni	0.598	0.092
Co	-0.585	0.703
Ba	0.647	0.065
Sr	0.783	-0.372
Cr	0.615	0.101
V (ppm)	-0.343	0.816

Correlation of various elements down the sediment column

To unravel the geochemical pattern and behaviour of seabed sediments off Rushikulya River, correlation of the major oxides and trace elements from VC-05 and VC-06 was undertaken. In VC-05, a strong positive correlation among Al₂O₃, Fe₂O₃, MgO, Na₂O, K₂O and P₂O₅ was observed, whereas a negative/poor correlation among MnO as well as CaO and the above-mentioned oxides were documented (Table 4). This is in contrast to the strong correlation between CaO, TiO₂ and MnO. In trace elements, Cu, Pb, Co, V and Zn were positively correlated to each other, while Ni was strongly correlated with Pb and negatively correlated with Cu and Zn (Table 5). Furthermore, Ba was strongly correlated with Sr and in turn with CaO down the sediment core. Albeit in VC-06, the correlation aspect was more or less similar to VC-05, critical differences included positive correlation of MnO with major oxides and a rather poor/negative correlation

between P₂O₅ and other oxides (Table 6). In addition to Cu, Pb, Zn, Co and V, C and Ni were positively correlated with each other (Table 7). Ni showed strong positive correlation with Pb and negative correlation with Cu and Zn, while Ba was strongly correlated with Sr and Zn.

Principal component analysis of major oxides and trace elements

Major oxides and trace elements in the core VC/1/2 accounted for 60.21% of the variance from 19 variables in the original dataset. Table 8 provides the factor loadings of the measured major oxides along with trace elements. The first axis (F1) explains 39.49% of the total variance, whereas the second PCA axis (F2) explains 20.72% of the total variance in the core VC/5 (Figure 3). The F1 axis shows high positive factor loading for Al₂O₃ (%), Fe₂O₃ (%), MgO (%), Na₂O (%), K₂O (%), P₂O₅ (%), Ni, Ba, Sr and Cr. On the other hand, the same axis depicts a low positive value for CaO (%), MnO (%), TiO₂ (%) and Pb. Negative and positive side of PCA axes F1 and F2 respectively, are marked by high loading of Cu, Zn, Co and V corresponding to the metals adsorbed into the clay fraction of the estuarine sediments. The second axis (F2) represents the dual source of calcium-detrital and authigenic precipitation with intermediate positive and negative loadings for CaO (%) and Sr respectively.

REE chemistry of carbonaceous clay

The carbonaceous sediments from the mouth of the Rushikulya River exhibited higher REE content, i.e. Σ REE varied between 204.38 and 288.45 ppm (Table 3). The LREE content in the analysed sediments ranged from 45.64 to 57.01 ppm for La, 84.21 to 118.48 ppm for Ce, 9.77 to 14.26 ppm for Pr, 33.41 to 49.83 ppm for Nd and 1.38 to 1.92 ppm for Eu. The MREEs such as Sm (6.51–9.55 ppm), Gd (7.06–9.23 ppm), Tb (0.99–1.24 ppm) and Dy (5.41–6.93 ppm) as well HREEs, viz. Ho (0.99–1.30 ppm), Er (2.86–3.77 ppm), Tm (0.52–0.61 ppm), Yb

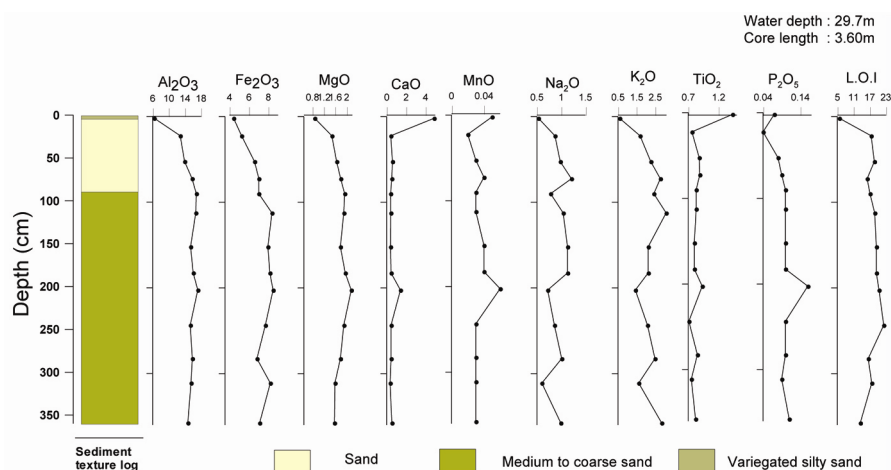


Figure 4. Downcore variation of sediment texture and major oxides of VC-05.

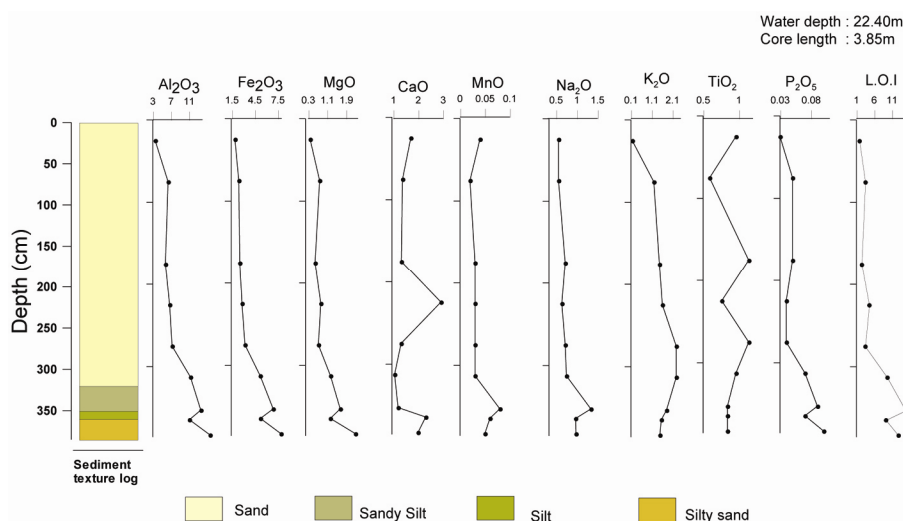


Figure 5. Downcore variation of sediment texture and major oxides of VC-06.

(2.89–3.74 ppm) and Lu (0.50–0.60 ppm) were at par with shale-normalized REE ratio of 1. Overall, the PAAS-normalized REE pattern was slightly LREE-enriched when compared to HREE with a prominent Ho anomaly.

Discussion

Overall, the major and trace elements in the sediments showed a significant correlation with aluminium. Further, on account of the fact that aluminium is responsible for the variation in other elements, except calcium and barium, it confirms the association of these elements with aluminosilicate minerals¹⁷. Positive correlation of iron with aluminium ($R_2 = 0.84–0.99$), and negative correlation with Ca, Sr and Ba negate the importance of iron oxides with respect to organic matter concentration. Furthermore, the low factor loading for CaO (%), MnO (%), TiO₂ (%) and Pb on F1 axis compared to the other elements can be attributed to its possible dual sources.

Hence, the present study indicated that the Al₂O₃ content of the sediments in both the cores was mostly derived from the aluminous clay minerals, whereas the Fe₂O₃ content accounted for the presence of Fe-bearing mineral phases (pyroxenes, amphiboles, garnets and magnetite). In VC-05, K was strongly correlated with Al ($R_2 = 0.67$) than VC-06 ($R_2 = 0.48$), and it was vice versa for Na. This strongly suggests the exclusive control of minerals, especially feldspar rather than clay minerals on the distribution of Na and K coupled with the fact that the cores were collected from the mouth of Rushikulya River. The higher TiO₂ concentration in the sediments of VC-06 which contains more sand than VC-05 and higher concentration near the coast than the deeper parts of the survey area can be attributed to higher concentration of Ti-rich heavy minerals in the sediments by the current activity¹⁸. Dominant presence of rutile in heavy mineral studies on the samples of the core VC-06 also augment this conclusion. A negative correlation between Ca and Al in both

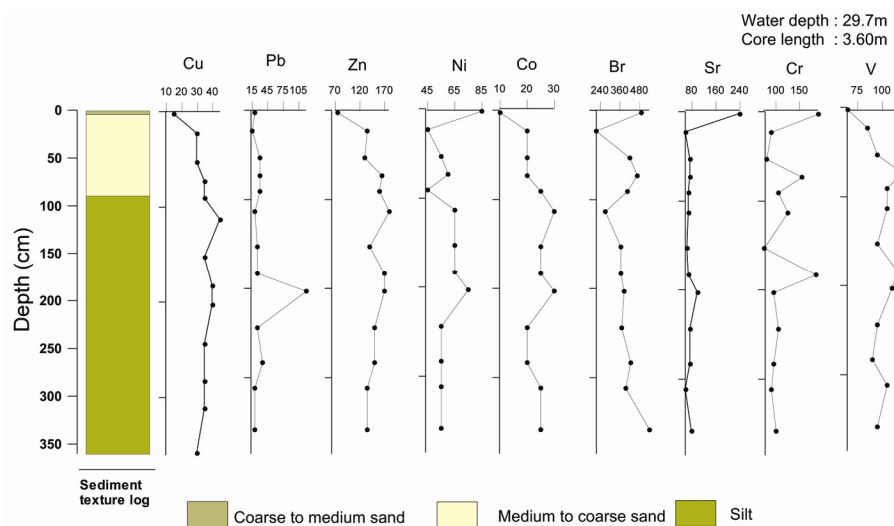


Figure 6. Downcore variation of sediment texture and trace elements of VC-05.

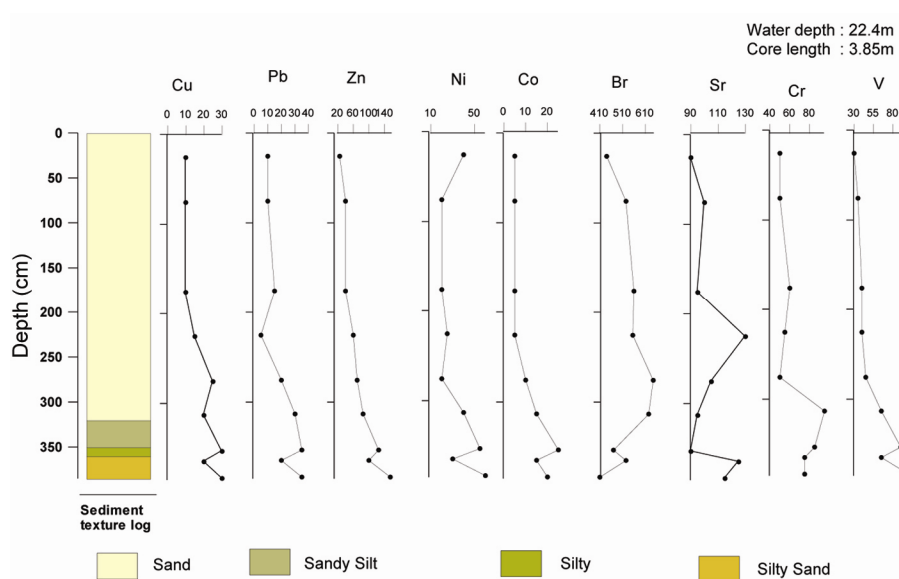


Figure 7. Downcore variation of sediment texture and trace elements of VC-06.

the cores indicate that CaO dominantly occurred within carbonates, thereby precluding the significant presence of CaO-bearing silicates¹⁹. The positive correlation between Mg and transition trace elements, such as Cr, Ni, Co and V indicated the presence of chlorite in the sediments derived from weathering of mafic rocks. In the present study, the poor association of Ba with other elements (Al, Fe, Mg, Ca, Mn, Na, K, Ti and P) could be due to its presence as only a minor host phase in the sediments of the survey area.

Down the cores of VC-05 and VC-06, Mg in the sediments was largely contributed by Fe-rich minerals (preferentially biotite and chlorite), as MnO followed the downcore path of both Al₂O₃ and Fe₂O₃ (Figures 4 and 5). Lack in correlation between CaO and MnO strength-

ens this argument and discards the MgO contribution in the sediments due to biogenic carbonates. In the context of the argument by Alagarsamy and Zhang¹⁶ of direct correlation between CaO and Co, the downcore variation trend in VC-06 suggested their contribution from organic matter content due to remineralization in the sediments. As these two cores were collected from the mouth of Rushikulya River where terrigenous sediments are the predominant contributors, the low value of P₂O₅ could be due to lithic minerals, viz. quartz, feldspar and biotite as deciphered from coarse fraction studies on these two cores, which contain less phosphorus (<0.03% P). Ba enrichment was mainly due to segregation from the ocean water by organic-rich sediments, either by adsorption or by the formation of BaSO₄ crystals in reducing

micro-environments. Thus, the higher Ba content in VC-05 can be explained by enrichment of organic matter (decayed wood) throughout the core than VC-06 (Figures 6 and 7). High Cr contents in VC-06 in sandy silt and silty regime can be attributed to clay-minerals (illite) that trap Cr in strongly reducing environments²⁰. Rather high concentration of Ni in organic-rich sediments of VC-05 down the profile than VC-06 could be due to the connection between Ni and marine organic matter and its increased tendency to bind to metals in sulphides (could be detrital pyrite) in the present case¹⁶. In contrast to the general tendency of lower Ni content on the surface sediments than below the surface observed in the analysed core, the close similarity of the Zn with Ni down the trace element profile is related to the nutrient cycle (H₄SiO₄) prevalent in the study area^{21,22}. On the whole, the trace elemental association indicated a reducing environment of deposition.

Usually, the dissolved REE entering the ocean is slightly enriched in the both LREE and HREE with

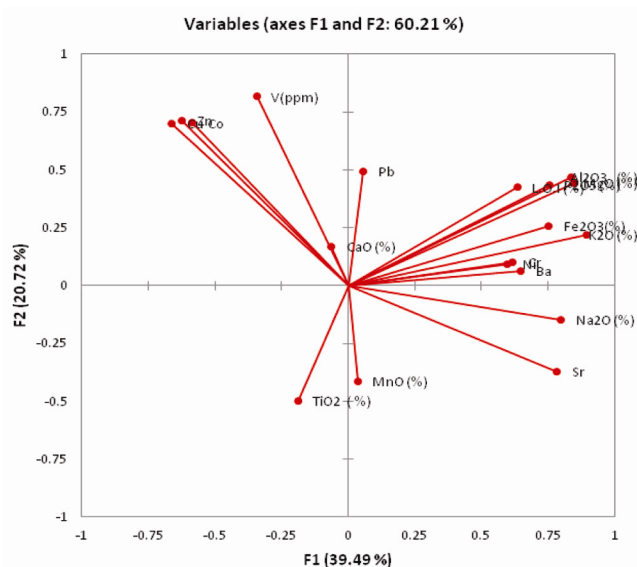


Figure 8. Biplot of F1 axis versus F2 axis based on principal component analysis of major oxides and trace elements from VC-05.

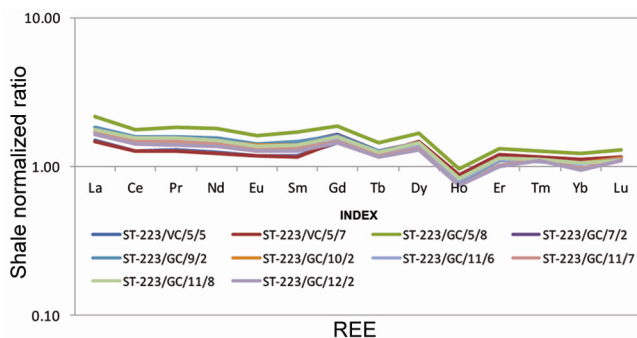


Figure 9. Post-Archean average shale (PAAS) normalized REE pattern of carbonaceous clay from the mouth of Rushikulya River.

respect to MREE²³. The slightly LREE-enriched shale normalized pattern of carbonaceous clay collected off Rushikulya River indicated adsorption of REE from the sea water into the carbonaceous clay without much differentiation (Figure 9). In addition, as suggested by Martin *et al.*²³ and Shimizu and Masuda²⁴, absence of Ce anomaly in the sediments also precluded the differential partitioning of individual REE. The enrichment of LREE relative to HREE could be explained by the preferential incorporation of LREE into the biogenic and hydrogenous phases in the study area. Hence, REE pattern of the sediments reflects that of sea water with REE removed from solution and incorporated into the sediments in an estuarine environment. Above this, the higher Σ REE content indicated its adsorption into clays, such as lacustrine clays as suggested by Roaldset and Rosenqvist²⁵.

The fundamental properties as well as two simultaneous mechanisms are believed to control the distribution of REE in sea water and ultimately in the seabed sediments²⁶. Most importantly, mechanisms for the differential concentration of REE are the association with calcareous skeletal material and absorptive scavenging by the settling particles. In the present study, a strong preferential uptake of Gd in calcareous skeletal material has been considered as one of the important mechanisms for positive anomaly in the sediments. This argument is even strengthened by the enriched presence of calcareous debris material in the sediments of the present study area. Additionally, because of the half-filled electron shell of Gd, solution and surface complexation of Gd relative to Tb (refs 27, 28), the surface sediments showed a relative Tb negative anomaly. The scavenging model of Byrne and Kim²⁷ suggested that Ho and neighbouring REEs formed considerably stronger surface complexes on the marine precipitates. Negative anomaly in the PAAS-normalized REE pattern in the marine sediments indicated the absence of such precipitates in the present study area. All these anomalies present in the late Holocene sediments of the study area are in tandem with the modern-day seabed sediments.

Conclusion

Geochemical analysis (major and trace elements) of seabed sediments of the inner to middle shelf region of the central part of the east coast of India, immediately near the growing spit of the Rushikulya River mouth showed a significant correlation with aluminium. In addition, the variation in other elements, except calcium and barium due to aluminium confirmed the association of these elements with aluminosilicate minerals. The higher concentration of Ti-rich heavy minerals near the coast in front of the Rushikulya River was inferred due to terrigenous supply by this river. The enrichment of Σ REE in the sediments can be interpreted as due to the absorption of REE

into the lattices of clays from seawater. Evidences such as intermittent layers of carbonaceous clay with abundant wood pieces, presence of H₂S and the enrichment of REE point towards the presence of a buried estuary.

1. Haq, B. U., Hardenbol, J. and Vail, P. R., Chronology of fluctuating sea levels since the Triassic (250 million years ago to present). *Science*, 1987, **235**, 1156–1167.
2. Vail, P. R. *et al.*, Seismic stratigraphy and global changes of sea level. In *Seismic Stratigraphy—Applications to Hydrocarbon Exploration* (ed. Payton, C. E.), American Association of Petroleum Geologist Memoir, 1977, vol. 26, pp. 49–212.
3. Banerjee, A. and Sengupta, R., Evidences of low stands on the Continental shelf of East coast of India. *Geol. Surv. India, Spl. Publ.*, 1992, **29**, 163–170.
4. Banerjee, P. K., Holocene and Late-Pleistocene relative sea level fluctuation along the east coast of India. *Mar. Geol.*, 2000, **165**, 243–260.
5. Mohapatra, G. P., Rao, B. R. and Biswas, N. R., Morphology and surface sediments of the eastern continental shelf off peninsular India. *Geol. Surv. India, Spl. Publ.*, 1992, **29**, 229–243.
6. Mil-Homens, M., Stevens, R. L., Abrantes, F. and Cato, I., Heavy metal assessment for surface sediments from three areas of the Portuguese continental shelf. *Continental Shelf Res.*, 2006, **26**, 1184–1205.
7. Kolla, V., Kostecki, J. A., Robinson, F., Biscaye, P. E. and Ray, P. K., Distribution and origin of clay minerals and quartz in surface sediments of the Arabian Sea. *J. Sediment. Petrol.*, 1981, **51**, 563–569.
8. Kolla, V. and Biscaye, P. E., Distribution and origin of quartz in the sediments of the Indian Ocean. *J. Sediment. Petrol.*, 1977, **47**, 642–649.
9. Kolla, V., Henderson, L. and Biscaye, P. E., Clay mineralogy and sedimentation in the western Indian Ocean. *Deep-Sea Res.*, 1976, **23**, 949–961.
10. Kolla, V., Ray, P. K. and Kostecki, J. A., Surficial sediments of the Arabian Sea. *Mar. Geol.*, 1981, **41**, 183–204.
11. Paropkari, A. L., Geochemistry of sediments from the Mangalore–Cochin shelf and upper slope of southwest India: geological and environmental factors controlling dispersal of elements. *Chem. Geol.*, 1990, **81**, 99–119.
12. Shankar, R., Subbarao, K. V. and Kolla, V., Geochemistry of surface sediments from the Arabian Sea. *Mar. Geol.*, 1987, **76**, 253–279.
13. Siddique, H. N. and Choudhury, A. N., The distribution of phosphates in some samples of the shelf sediments of the west coast of India. *Bull. Natl. Inst. Sci. India*, 1968, **38** (Part 1), 483–490.
14. Murty, P. S. N., Rao, Ch. M. and Reddy, C. V. G., Partition patterns of iron, manganese, nickel and cobalt in the sediments of the west coast of India. *Indian J. Mar. Sci.*, 1973, **2**, 6–12.
15. Manjunatha, B. R. and Shankar, R., The influence of the rivers on the geochemistry of shelf sediments, southwestern coast of India. *Environ. Geol.*, 1997, **31**, 107–116.
16. Alagarsamy, R. and Zhang, J., Geochemical characterization of major and trace elements in the coastal sediments of India. *Environ. Monit. Assess.*, 2010, **161**(1–4), 161–176.
17. Rubio, B., Nombela, M. A. and Vilas, F., Geochemistry of major and trace elements in sediments of the Ria de Vigo (NW Spain): an assessment of metal pollution. *Mar. Pollut. Bull.*, 2000, **40**, 968–980.
18. Shimmield, G. B., Price, N. B. and Pedersen, T. F., The influence of hydrography, bathymetry and productivity on sediment type and composition of the Oman Margin and in the northwest Arabian Sea. In *The Geology and Tectonics of the Oman Region* (eds Robertson, A. H. F., Searle, M. P. and Ries, A. C.), Geological Society Special Publication, 1990, pp. 759–769.
19. Bianchini, G., Laviano, R., Lovo, S. and Vaccaro, C., Chemical–mineralogical characterization of clay sediments around Ferrara (Italy): a tool for an environmental analysis. *Appl. Clay Sci.*, 2002, **21**(3–4), 165–176.
20. Turekian, K. K. and Wedepohl, K. H., Distribution of the elements in some major units of the Earth's crust. *Bull. Geol. Soc. Am.*, 1961, **72**(2), 175–192.
21. Broecker, W. S. and Peng, T.-H., *Tracers in the Sea*, Eldigio Press, New York, USA, 1982.
22. Bruland, K. W., Oceanographic distributions of cadmium, zinc, nickel and copper in the North Pacific. *Earth Planet. Sci. Lett.*, 1980, **47**, 176–198.
23. Martin, J. M., Hogdal, O. and Philipott, S. C., Rare earth element supply to the ocean. *J. Geophys. Res.*, 1976, **81**, 3119–3124.
24. Shimuzu, H. and Masuda, A., Cerium in chert as an indication of marine environment of its formation. *Nature*, 1977, **266**, 346–348.
25. Roaldset, E. and Rosenqvist I. Th., Rare earth elements in vivianite from Lake Asrum. *Lithos*, 1971, **4**, 417–422.
26. De Baar, H. J. W., Bacon, M. P., Brewer, P. G. and Bruland, K. W., Rare earth elements in the Atlantic and Pacific Oceans. *Geochim. Cosmoch. Acta*, 1985, **49**, 1943–1959.
27. Byrne, R. H. and Kim, K.-H., Rare earth element scavenging in seawater. *Geochim. Cosmochim. Acta*, 1990, **54**, 2645–2656.
28. Byrne, R. H. and Li, B., Comparative complexation behaviour of the rare earths. *Geochim. Cosmochim. Acta*, 1995, **59**, 4575–4589.

Received 9 July 2016; revised accepted 10 February 2017

doi: 10.18520/cs/v112/i12/2424-2433